JOURNAL OF GEOPHYSICAL RESEARCH, VOL. 87, NO. B5, PAGES 3893–3904, MAY 10, 1982

Absorption Band Q Model for the Earth

DON L. ANDERSON AND JEFFREY W. GIVEN

Seismological Laboratory, California Institute of Technology, Pasadena, California 91125

Body wave, surface wave, and normal mode data are used to place constraints on the frequency dependence of Q in the mantle. With a simple absorption band model it is possible to satisfy the shear sensitive data over a broad frequency range. The quality factor $Q_s(\omega)$ is proportional to ω^α in the band and to ω and ω^{-1} at higher and lower frequencies, respectively, as appropriate for a relaxation mechanism with a spectrum of relaxation times. The parameters of the band are $Q(\text{min}) = 80$, $\alpha = 0.15$, and width, 5 decades. The center of the band varies from 10^1 seconds in the upper mantle, to 1.6×10^3 seconds in the lower mantle. The shift of the band with depth is consistent with the expected effects of temperature, pressure and stress. High Q_s regions of the mantle are attributed to a shift of the absorption band to longer periods. To satisfy the gravest fundamental spheroidal modes and the *ScS* data, the absorption band must shift back into the short-period seismic band at the base of the mantle. This may be due to a high temperature gradient or high shear stresses. A preliminary attempt is also made to specify bulk dissipation in the mantle and core. Specific features of the absorption band model are low Q in the body wave band at both the top and the base of the mantle, low Q for long-period body waves in the outer core, an inner core Q_s that increases with period, and low Q_p/Q_s at short periods in the middle mantle. The short-period Q_s increases rapidly at 400 km and is relatively constant from this depth to 2400 km. The deformational Q of the earth at a period of 14 months is predicted to be 463.

INTRODUCTION

Attenuation in solids and liquids, as measured by the quality factor Q, is typically frequency dependent. In seismology, however, Q is usually assumed to be independent of frequency. The success of this assumption is a reflection of the limited precision, resolving power and bandwidth of seismic data and the trade-off between frequency and depth effects rather than a statement about the physics of the earth's interior.

The theory of seismic attenuation has now been worked out in some detail [*Anderson,* 1980; *Anderson and Minster,* 1979, 1980; *Minster and Anderson,* 1980, 1981]. Although a mild frequency dependence of Q can be expected over a limited frequency band, Q or Q^{-1} should be a linear function of frequency at greater and lower frequencies.

In this paper we apply the absorption band concept [*Liu et al.,* 1976; *Kanamori and Anderson,* 1977; *Anderson et al.,* 1977; *Anderson and Minster,* 1980; *Minster and Anderson,* 1981] to the attenuation of body waves, surface waves, and free oscillations. The basic method is described by *Anderson and Hart* [1978*a*, *b*] except that we replace the frequency-independent Q assumption with the absorption band assumption. We make the very restrictive assumption that the shape of the band is invariant with depth and only the location varies.

The frequency-independent Q models, such as SL8 [*Anderson and Hart,* 1978*b*] provide an adequate fit to the normal model data. There is increasing evidence, however, that short-period body waves may require higher Q values [*Der and McElfresh,* 1980; *Sipkin and Jordan,* 1979; *Lundquist and Cormier,* 1980; *Clements,* 1982]. Some geophysical applications require estimates of the elastic properties of the earth outside the seismic band. These include calculations of tidal Love numbers, Chandler periods, and high-frequency moduli for comparison with ultrasonic data. The constant Q models cannot be used for these purposes. There is also no current model that reconciles the normal mode and body wave data. For these reasons it is important to have a physically sound attenuation model for the earth, and this is the primary motivation for the present paper. Our present goal is simply to develop such a model. The pertinent data, including a discussion of uncertainties, has been assembled by *Anderson and Hart* [1978*a*, *b*]. The data set has been updated for the present study.

Copyright 1982 by the American Geophysical Union.

Paper number 2B0308.
0148-0227/82/002B-0308$05.00

THEORY

For a solid characterized by a single relaxation time τ, Q^{-1} is a Debye function with maximum absorption at $\omega\tau = 1$. For a solid with a spectrum of relaxation times the band is broadened, and the maximum attenuation is reduced [*Kanamori and Anderson,* 1977; *Anderson and Minster,* 1980]. For a polyscrystalline solid with a variety of grain sizes, orientations, and activation energies the absorption band can be appreciably more than several decades wide. If, as seems likely, the attenuation mechanism in the mantle is an activated process, the relaxation times should be a strong function of temperature and pressure. The location of the absorption band, therefore, changes with depth. The theory of attenuation in fluids [*Anderson,* 1980] indicates that Q in the outer core should also depend on frequency.

Theoretical considerations indicate that Q can be a weak function of frequency only over a limited bandwidth. If the material has a finite elastic modulus at high frequency and a nonzero modulus at low frequency there must be high- and low-frequency cutoffs in the relaxation spectrum. Physically, this means that relaxation times cannot take on arbitrarily high and low values. The relationship between Q and bandwidth [*Kanamori and Anderson,* 1977] indicates that a finite Q requires a finite bandwidth of relaxation times and therefore an absorption band of finite width. Q can be a weak function of frequency only in this band.

Anelastic attenuation in solids and liquids having a single characteristic relaxation time satisfies the Debye equation

$$Q_{(\omega)}^{-1} = 2Q_m^{-1} \frac{\omega\tau}{1 + \omega^2\tau^2} \tag{1}$$

where Q_m^{-1} is the maximum or peak absorption. Crystalline solids typically have a distribution of relaxation times, $D(\tau)$, giving

$$Q^{-1}(\omega) = 2\int_0^\infty Q_m^{-1} D(\tau) \frac{\omega\tau}{1+\omega^2\tau^2} d\tau \qquad (2)$$

For an appropriate choice of $D(\tau)$ this yields an absorption band in which $Q(\omega)$ is slowly varying between τ_1 and τ_2, the minimum and maximum relaxation times in the spectrum. The theory of the absorption band and its relationship to mantle rheology has been developed by *Minster and Anderson* [1981].

A distribution function of the form

$$D(\tau) \sim \tau^{\alpha-1} \qquad (3)$$

with cutoffs at τ_1 and τ_2 gives

$$Q(\omega) \sim \omega^\alpha = (2\pi f)^\alpha$$

in the absorption band and $Q(\omega) \sim \omega^{\pm 1}$ outside the band.

We approximate the absorption band in the following way:

$$Q = Q_m (f\tau_2)^{-1} \qquad f < 1/\tau_2$$

$$Q = Q_m (f\tau_2)^\alpha \qquad 1/\tau_2 < f < 1/\tau_1$$

$$Q = Q_m(\tau_2/\tau_1)^\alpha (f\tau_1) \qquad f > 1/\tau_1$$

where f $(= \omega/2\pi)$ is the frequency, τ_1 is the short-period cutoff, τ_2 is the long-period cutoff, and Q_m is the minimum Q which occurs at $f = 1/\tau_2$ if $\alpha > 0$. These parameters are shown in Figure 1.

Effect of T, P, and Stress

The relaxation time τ for an activated process depends exponentially on temperature and pressure:

$$\tau = \tau_0(z) \exp[(E^* + PV^*)/RT]$$

where E^* and V^* are activation energy and volume, respectively. The characteristic time τ_0 depends on l^2 and D for diffusion-controlled mechanisms, where l and D are a characteristic length and a diffusivity, respectively. Characteristic lengths, such as dislocation or grain size, are a function of tectonic stress which is a function of depth z. The location of the band therefore depends on tectonic stress, temperature, and pressure. The width of the band is controlled by the distribution of relaxation times which in turn depends on the distribution of grain sizes or dislocation lengths.

With an activation energy of 60 kcal/mol, τ decreases by about an order of magnitude for a temperature rise of 200°C. An activation volume of 10 cm^3/mol causes τ to increase by an order of magnitude for a 30-kbar increase in pressure. In regions of low temperature gradient the maximum absorption shifts to longer periods with increasing depth. This condition is probably satisfied throughout most of the mantle except in thermal boundary layers. Characteristic lengths such as grain size and dislocation length decrease with increasing stress. A decrease in tectonic stress by a factor of 3 increases the relaxation time by about an order of magnitude [*Anderson and Minster,* 1980]. A decrease of stress with depth moves the absorption band to longer periods.

The effect of pressure dominates over temperature for most of the upper mantle [*Minster and Anderson,* 1981], and tectonic stress probably decreases with depth. Therefore the absorption band is expected to move to longer periods with increasing depth. A reversal of this trend may be caused by high-stress or high-temperature gradients across boundary layers or by enhanced diffusion due to changes in crystal structure or in the nature of the point defects.

Procedure

The parameters of the absorption band are (1) minimum Q, Q_m, (2) short-period corner τ_1, (3) long-period corner τ_2, and (4) the frequency dependency of Q in the absorption band, i.e., $Q \sim \omega^\alpha$. For a given physical mechanism there are relationships between the width of the band (τ_2/τ_1), Q_m, and α, i.e., these three parameters are not independent [*Minster and Anderson,* 1981]. For fixed α, τ_2/τ_1 increases as Q_m^{-1} decreases. We assume that the parameters of the absorption band, Q_m^{-1}, τ_1/τ_2, and α, are constant throughout the mantle and use the seismic data to determine the location of the band as a function of depth, i.e., $\tau_1(z)$. This assumption is equivalent to assuming that the activation energy E^* and activation volume V^* are fixed. By assuming that the characteristics of the absorption band are invariant with depth we are assuming that the width of the band is controlled by a distribution of characteristic relaxation times rather than a distribution of activation energies. Although this assumption can be defended to some extent, it has been introduced to reduce the number of model parameters. If a range of activation energies is assumed, the shape of the band (i.e., width and height) varies with temperature and pressure.

In setting up the starting model we used the following considerations:

1. Body waves traverse the lower mantle with little attenuation. On the other hand, the normal modes require a relatively low-Q lower mantle [*Sailor and Dziewonski,* 1978; *Anderson and Hart,* 1978*b*]. This suggests that the absorption band in the lower mantle is centered at long periods.

2. The upper mantle is highly attenuating for both surface waves and body waves, although there is some evidence for an increase in Q at very short periods. The absorption band in the upper mantle therefore occurs at shorter periods than in the lower mantle, but τ_1 is larger than the periods of short-period body waves.

3. At body wave periods the Q is large in the outer core and small in the inner core [*Sacks,* 1972; *Doornbos,* 1974; *Cormier and Richards,* 1976]. We assume that the short-period Q decreases with depth throughout the core.

4. The observation of core modes requires that Q of the inner core be high at normal mode periods. The radial modes imply a high-Q outer core [*Anderson and Hart,* 1978*a*, *b*]. We assume therefore that the core behaves as a classic fluid, with $Q \sim \omega^{-1}$, at long periods [*Anderson,* 1980].

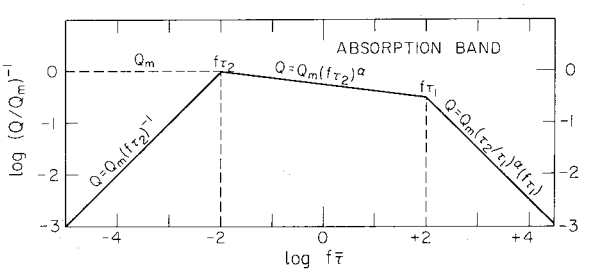

Fig. 1. Schematic illustration of the absorption band. For shear wave attenuation in the mantle Q_m, α and τ_2/τ_1 are fixed and τ_1 is found as a function of depth from the seismic data.

TABLE 1. Absorption Band Parameters for Q_s

Radius, km	τ_1,s	τ_2/τ_1	Q_s, min (τ_1)	Q_s, 100 s	α
1230	0.14	2.43	35	1000	0.15
3484	...	...	...	...	—
4049	0.0025	10^5	80	92	0.15
4832	25.2	10^5	80	366	0.15
5700	12.6	10^5	80	353	0.15
5950	0.0031	10^5	80	330	0.15
6121	0.0009	10^5	80	95	0.15
6360	0.0044	10^5	80	90	0.15
6371	0	∞	500	500	0

Q_m is found from the minimum Q modes, i.e., mantle Love and Rayleigh waves, and is assumed to be constant with depth. The parameters α and τ_1 were estimated from data that sample the midmantle at various frequencies. This part of the mantle is high Q for body waves but low Q at normal mode periods. This suggests that the high-frequency end of the band occurs at intermediate periods. To satisfy the relatively low Q of long-period ScS [*Sipkin and Jordan,* 1979], the absorption band has to be shifted to higher frequencies at the base of the mantle. Then τ_2 is determined from ${}_0S_2$ to ${}_0S_5$, which are sensitive to Q_s at the base of the mantle. With Q_m, α, τ_1, and τ_1/τ_2 fixed, the full data set is used to adjust $\bar{\tau} = (\tau_1\tau_2)^{1/2}$, i.e., the geometric mean location of the absorption band as a function of depth. The fixed parameters of the band, found by the above procedure, are $\alpha = 0.15$ and $Q_m = 80$. A similar procedure is used to estimate Q_s in the inner core. The parameters of the absorption bands are given in Tables 1 and 2. The locations of the bands as a function of depth are shown in Figures 2–4. We will refer to the absorption band model as ABM.

The Mantle

The variation of τ_1 and τ_2 with depth in the mantle is shown in Figure 2. Note that $\bar{\tau}$ decreases with depth in the uppermost mantle. This is expected in regions of high thermal gradient; $\bar{\tau}$ increases slightly below 250 km and abruptly at 400 km. In the early iterations it was assumed that any abrupt change in $\bar{\tau}$ would occur at 670 km, but this is clearly too deep. Apparently, a high-temperature gradient and high tectonic stresses can keep the absorption band at high frequencies throughout most of the upper mantle, but these effects are overridden below 400 km, where most mantle minerals are in the cubic structure. A phase change, along with high pressure and low stress, may contribute to the lengthening of the relaxation times. Note that $\bar{\tau}$ changes only slightly through most of the lower mantle.

The location of the absorption band is almost constant

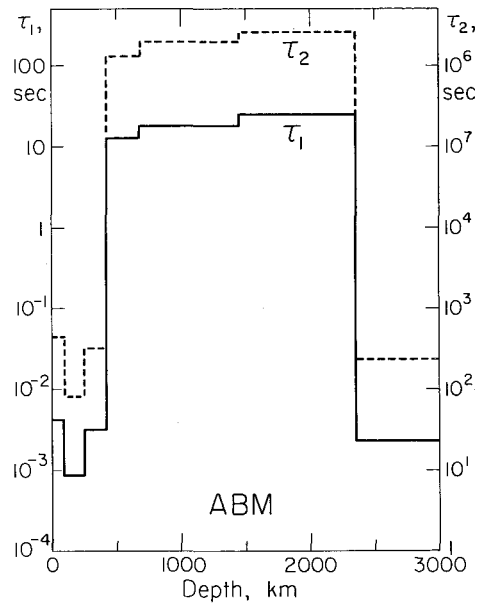

Fig. 2. The characteristic times τ_1 and τ_2 as a function of depth in the mantle for ABM for Q_s.

from a depth of about 400 to 2000 km (Figure 2). Most of the lower mantle therefore has high Q_s for body waves and low Q_s for free oscillations. In the initial models the location of the absorption band was kept constant from a depth of 2000 km to the core mantle boundary. Since Q decreases with period in the band, these models gave very low Q values for the low-order long-period modes. The low-order spheroidal modes apparently require a distinctly different location for the absorption band in the lower 500 km of the mantle. These data can be satisfied by moving the band to the location shown in the lower part of Figure 3. This gives a low-Q region at the base of the mantle at body wave periods (region D″ in Figure 4).

The average mantle Q_s for this model is 280 at 10 s, and 176 at 100 s (Table 3), which is in good agreement with the ScS data [*Anderson and Hart,* 1978*a*; *Nakanishi,* 1979*b*; *Sipkin and Jordan,* 1979].

Note that the location of the absorption band in the lowermost mantle is similar to the location in the uppermost mantle (Figure 3 and Table 4). A low-Q zone at the base of the mantle, at body wave periods, has been proposed before (see *Anderson and Hart* [1978*a*, *b*] for summaries). Free oscillation data alone do not require such a zone if Q is assumed to be independent of frequency [*Sailor and Dziewonski,* 1978; *Dziewonski and Anderson,* 1981], but it cannot be ruled out either [*Anderson and Hart,* 1978*a*]. A low-Q zone, for body waves, is a prediction of the present

TABLE 2. Relaxation Times (τ_1, τ_2) and Q_K for Bulk Attenuation at Various Periods Q_K (min) = 400, $\alpha = 0.15$

			Q_K			
	τ_1, s	τ_2, s	$T = 1$ s	$T = 10$ s	$T = 100$ s	$T = 1000$ s
Upper mantle	0	3.33	479	1200	1.2×10^4	1.2×10^5
Lower mantle	0	0.20	2000	2×10^4	2×10^5	2×10^6
Outer core	15.1	66.7	7530	753	600	6,000
	9.04	40.0	4518	493	1000	10,000
Inner core	3.01	13.3	1506	418	3000	3×10^4

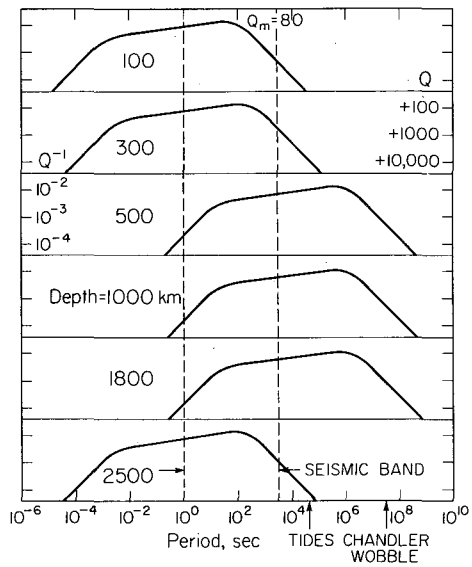

Fig. 3. The location of the absorption band for Q_s as a function of depth in the mantle.

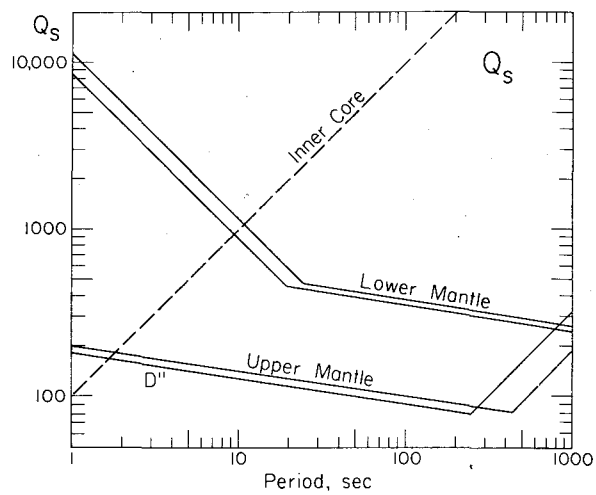

Fig. 4. Q_s as a function of period for the mantle and inner core for ABM. Note the similarity of the upper mantle and the lowermost mantle (D''). These may be thermal (high-temperature gradient) and mechanical (high stress) boundary layers associated with mantle convection.

modeling and results from the need to increase the Q at the base of the mantle at periods greater than 1000 s.

The need for a shift of the absorption band in the lowermost mantle can be seen from Table 5. PREM is a frequency-independent Q model with Q_s = 312 throughout the lower mantle [*Dziewonski and Anderson,* 1981]. The PREM Q values are similar to those of ABM for periods between 100 and 600 s, a period range controlled by the upper and middle mantle. Most of the normal mode data is in this period range. For PREM, model Q values increase only gradually with a further increase in period, and for ${}_0S_2$ to ${}_0S_4$ the PREM values are at the lower end of the data range and much lower than values from ABM. These modes are sensitive to Q_s at the base of the mantle. If Q_s decreases with period from 1000 to >3232 s, as in the midmantle (Figure 3), then the low-order modes would have even lower Q. By shifting the peak absorption to shorter periods the Q of the low-order modes can be satisfied.

In the frequency-independent Q models (Table 5), Q increases slowly from ${}_0S_8$ to ${}_0S_3$ and is still relatively low at ${}_0S_2$. If the Q in the lower mantle decreases with period, as in the absorption band model, and the location of the absorption band is constant throughout the lower mantle, then the Q of modes ${}_0S_7$ to ${}_0S_4$ would be about 320, and ${}_0S_2$ would be less than 400. Even though there is a large uncertainty in the Q of modes ${}_0S_2$ to ${}_0S_4$, such low values are not favored by the majority of the data.

The parameter α was initially set to 0.3 [*Anderson and Minster,* 1979], but we were not able to match the data with this strong a frequency dependence in the absorption band. We found that α = 0.15 gave a satisfactory fit. We did not test lower values.

The Core

Under the normal conditions, fluids in general and molten metals in particular satisfy the relaxation equations with $\omega\tau \ll 1$ giving $Q \sim \omega^{-1}$. Pressure serves to increase $\bar{\tau}$, and the high absorption of short-period P waves in the inner core suggests that $\bar{\tau}$ may be of the order of 1 s in this region [*Anderson,* 1980]. The high Q of the outer core at body wave frequencies suggests that the absorption band is at longer or shorter periods.

Q in the core is assumed to be a Debye peak, which we approximate as a narrow absorption band with a fixed Q_m and width. With these assumptions we find Q_m = 400, and $\bar{\tau}$, the mean relaxation time, decreases with depth from 32 to 19 s in the outer core to 6 s in the inner core.

The net result is a slowly varying Q_p, 406 to 454, for the inner core between 0.1 to 10 s, increasing to 3320 at 100 s and 3.3×10^4 at 1000 s. Most studies of Q_p of the inner core at

TABLE 3. Average Mantle Q Values as Function of Period, Model ABM

	Period, s					
	0.1	1.0	4.0	10.0	100	1000
			Q_s			
Upper mantle	379	267	210	173	127	295
Lower mantle	1068	721	520	382	211	266
Whole mantle	691	477	360	280	176	274
			Q_p			
Upper mantle	513	362	315	354	311	727
Lower mantle	586	1228	1262	979	550	671
Whole mantle	562	713	662	639	446	687

Q (${}_0S_2$) at 3232 s is 596; at 12 hours, 514; at 14 months, 463.

TABLE 4. Q_s and Q_p as Function of Depth and Period for Model ABM

	Q_s				Q_p			
Depth, km	1 s	10 s	100 s	1000 s	1 s	10 s	100 s	1000 s
5142	100	1000	10,000	10^5	511	454	3322	3.3×10^4
4044	...	...	...	...	4518	493	1000	10^4
2887	...	...	...	...	7530	753	600	6000
2843	184	130	92	315	427	345	247	846
2400	184	130	92	315	427	345	247	846
2200	11,350	1135	366	259	2938	2687	942	668
671	8919	892	353	250	2921	2060	866	615
421	5691	569	330	234	741	840	819	603
421	190	134	95	254	302	296	244	659
200	157	111	90	900	270	256	237	2365
11	200	141	100	181	287	262	207	377
11	500	500	500	500	487	767	1168	1232

body wave frequencies give values between 200 and 600 [e.g., *Anderson and Hart,* 1978*b*]. In the outer part of the outer core, Q_p decreases from 7530 at 1 s to 753 at 10 s and then increases to 6000 at 1000 s. The relative location of the band is fixed by the observation that short-period P waves see a high-Q outer core and a low-Q inner core. The absorption band model predicts relatively low Q for 10- to 50-s P waves in the outer core. Data is sparse, but long-period P waves in the outer core may be attenuated more than short-period waves [*Suzuki and Sato,* 1970; *Qamar and Eisenberg,* 1974]. There are, however, complications in trying to interpret this data [*Cormier and Richards,* 1976; *Choy,* 1977]. The approach we take leads to the prediction that Q_s of the inner core is high at normal mode periods.

BULK ATTENUATION

The attenuation of shear waves, Love and Rayleigh waves, toroidal oscillations, and most of the spheroidal modes are controlled almost entirely by Q_s in the mantle. Once the mantle Q_s is determined, the Q of P waves and the high-Q spheroidal and radial modes can be used to estimate Q_K.

The relationship between Q_p, Q_s, and Q_K is

$$Q_p^{-1} = LQ_s^{-1} + (1 - L)Q_K^{-1}$$

where $L = (4/3)\ (\beta/\alpha)^2$ and β and α are the shear and compressional velocities. For a Poisson solid with $Q_K^{-1} = 0$,

$$Q_p = (9/4)Q_s$$

TABLE 5. Fundamental Spheroidal Mode Q

Mode	Period, s	ABM	SL8	PREM	Data
${}_0S_2$	3232	596	540	510	500–589
${}_0S_3$	2134	499	435	417	450–520
${}_0S_4$	1546	421	398	373	400–411
${}_0S_5$	1190	377	391	356	300–400
${}_0S_6$	964	350	391	347	343–399
${}_0S_7$	812	333	392	342	373–460
${}_0S_8$	708	323	388	337	295–357
${}_0S_9$	634	319	380	333	328
${}_0S_{10}$	580	319	368	328	320
${}_0S_{12}$	503	317	341	315	308
${}_0S_{14}$	448	307	313	298	294
${}_0S_{16}$	407	294	286	279	276
${}_0S_{18}$	374	276	262	259	282
${}_0S_{20}$	347	254	241	241	240
${}_0S_{22}$	325	231	222	225	228
${}_0S_{24}$	306	212	207	211	210
${}_0S_{26}$	290	198		200	198
${}_0S_{28}$	275	187		191	188
${}_0S_{30}$	262	177		183	179
${}_0S_{40}$	212	148	149	158	151
${}_0S_{50}$	178	136	136	143	137
${}_0S_{60}$	153	128	129	133	122
${}_0S_{70}$	134	121	125	126	120
${}_0S_{76}$	125	117			122
${}_0S_{80}$	119	114		122	
${}_0S_{90}$	107	107		119	
${}_0S_{100}$	97	100		118	
${}_0S_{110}$	88	93		118	
${}_0S_{120}$	81	94		119	
${}_0S_{130}$	75	95		121	
${}_0S_{140}$	70	96		124	
${}_0S_{150}$	66	97		128	

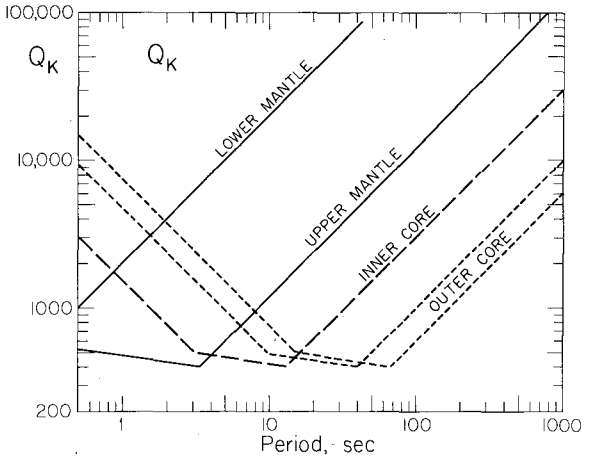

Fig. 5. Q_K as a function of frequency for various regions in the earth. There are two layers in the outer core (see Table 4).

The Q_p/Q_s ratio [e.g., 1967] can be used to estimate Q_K.

There is a small component of bulk dissipation associated with the shear deformation of polycrystalline material [*Budiansky and O'Connell,* 1980]. This amounts to about 2% of the shear dissipation and has the same frequency dependence. There is also a component of bulk dissipation in such material that is independent of the shear dissipation and which can be much larger. This is the intergranular thermoelasticity mechanism [*Zener,* 1948], a relaxation mechanism that depends on grain size and thermal conductivity and is only a weak function of temperature and pressure. This mechanism is predicted to be important at body wave frequencies [*Anderson,* 1980].

In fluids, bulk dissipation is controlled by viscosity and concentration fluctuations [*Anderson,* 1980], and again, the classic relaxation relations hold. Therefore the absorption band concept can be applied to bulk dissipation in both the mantle and core.

The main constraints on the bulk attenuation are provided by the low-order radial modes, the high-Q spheroidal modes, and short-period compressional waves. Bulk losses caused by bulk viscosity or intergranular thermal currents are relaxation mechanisms, and therefore, $Q_K \sim \omega^{-1}$ at long periods.

In general, bulk attenuation is less important than shear attenuation. The radial mode ${}_0S_0$ apparently requires bulk dissipation somewhere in the earth at a period of 1230 s [*Anderson and Hart,* 1978*a*, *b*; *Sailor and Dziewonski,* 1978]. *Kanamori* [1967] estimated Q_p/Q_s for the whole mantle from *ScS*, *ScP*, and *PcS* phases and obtained 1.9 in the period range 1.5 to 5 s. This is much less than the value which is expected if $Q_K^{-1} = 0$, and this implies a component of bulk attenuation at short periods. We assume that free oscillation periods are long compared to bulk relaxation times [*Anderson,* 1980], and therefore, $Q \sim \omega^{-1}$. The value of Q_K at long periods is estimated from the radial modes. With this procedure, however, the predicted Q_p for short-period body waves is distinctly too low. This implies that the minimum absorption, in the context of an absorption band model, occurs somewhere between the body wave and normal mode bands. By trial and error we found that a minimum Q_K of 400 could satisfy P wave observations for both the inner core and upper mantle. We adopted this value for the whole earth and found the location of the Q_K band. Values for τ_2, with this assumption, ranged from 0.2 to 67 s.

The variation of Q_K with frequency for the various regions of the earth is shown in Figure 5. The location of the lower mantle curve is dictated by the observation that both short-period P waves and the radial modes require a high-Q lower mantle. Low Q is predicted in this region for high-frequency P waves.

TABLE 6. Spheroidal Overtone Q

Mode	Period, s	ABM	SL8	PREM	Data
${}_1S_2$	1470	343			
${}_1S_4$	852	296			
${}_1S_7$	604	315	473		484*
${}_1S_{10}$	466	261			
${}_1S_{20}$	254	163			
${}_1S_{40}$	149	157			
${}_1S_{50}$	125	151			
${}_2S_2$	1049	6563			546
${}_2S_4$	726	411	544	380	350*–546
${}_2S_{10}$	416	221		181	
${}_2S_{15}$	309	161	252	258	244*
${}_2S_{23}$	202	118	407		514
${}_2S_{26}$	179	191	202	194	158–275
${}_2S_{30}$	161	200	179	181	150–207
${}_2S_{31}$	157	198	178	179	143
${}_2S_{39}$	131	188	169	168	179*
${}_2S_{57}$	98	170	160		174
${}_2S_{60}$	94	165	158	154	151*
${}_3S_1$	1061	856	902	827	1020*
${}_3S_2$	903	577		367	
${}_3S_6$	392	212		276	
${}_3S_{12}$	297	210	261	245	179–239
${}_3S_{13}$	285	214	255	241	227–271
${}_3S_{20}$	217	222	212	210	229*
${}_3S_{42}$	111	206	211	225	180

*See text.

TABLE 7. Spheroidal Overtone Q

Mode	Period, s	ABM	SL8	PREM	Data
${}_4S_3$	488	465	534	480	560
${}_4S_{14}$	225	189	296	264	288*
${}_4S_{19}$	192	218	294	259	291*
${}_4S_{21}$	181	231	291	259	275
${}_4S_{23}$	170	241	287	259	312
${}_4S_{25}$	161	248	281	258	260
${}_4S_{26}$	157	250	278	256	306
${}_4S_{31}$	139	246	258	252	264*
${}_4S_{32}$	136	244	254	251	299
${}_4S_{34}$	130	237	245	246	234*
${}_4S_{35}$	127	234	240	244	246*
${}_4S_{39}$	118	218	223	233	193
${}_5S_7$	304	480	—	493	496*
${}_5S_{22}$	154	212	303	—	306
${}_5S_{25}$	143	227	294	263	231
${}_5S_{26}$	140	233	291	260	236
${}_5S_{30}$	129	251	276	248	248*
${}_5S_{38}$	110	265	263	235	223*
${}_6S_1$	505	695	873	—	700
${}_6S_8$	268	189	263	—	286
${}_6S_9$	252	229	314	321	292*
${}_6S_{13}$	191	208	264	—	291
${}_6S_{23}$	138	272	325	292	299
${}_6S_{31}$	116	259	244	252	391
${}_6S_{36}$	106	282	247	250	342
${}_6S_{47}$	89	263	237	245	276

*See text.

A useful measure of body wave attenuation is the ratio of travel time to average Q along the path, or t^* [*Kovach and Anderson*, 1964]. If $t_p{}^*$ at short distances is to be as great as 0.6 to 1.0 s, then a compressional component of attenuation is required. With the Q_K band as shown, the $t_p{}^*$ at 1-s period and 30° distance is 0.65 s. No attempt was made to estimate τ_1, i.e., the short-period $Q_K{}^{-1}$ rolloff, for the mantle. This requires knowledge of Q_p as a function of frequency for periods shorter than about 1 s. If we assume that Q_K of the upper mantle is a simple Debye peak, then $Q_K \sim \omega$ at periods shorter than about 1 s. *Lundquist and Cormier* [1980] estimate that τ_1 is about 0.04 s for P waves in the upper mantle. On the other hand, τ_1 for Q_s in the upper mantle is about 0.3×10^{-2} to 10^{-3} s so that Q_p is expected to increase linearly with frequency only at very short periods.

The location of the Q_K band for the inner core is constrained by the low Q_p for short-period P waves. Q_K of the outer core is constrained by P waves and the radial modes. Note that Q_K, and therefore Q_p, is predicted to increase with period from about 50 s to longer periods. Relatively low Q, <500, is predicted between about 10 and 80 s. Measurements of the attenuation of long-period body waves in the outer

TABLE 8. Fundamental Toroidal Mode Q

Mode	Period, s	ABM	SL8	PREM	Data
${}_0T_2$	2631	268	272	250	250–400
${}_0T_3$	1702	269	257	240	325–400
${}_0T_4$	1304	267	241	228	290–425
${}_0T_5$	1076	265	224	216	185–280
${}_0T_6$	926	263	209	205	266–357
${}_0T_7$	818	259	195	196	125–141
${}_0T_8$	736	253	184	187	170–295
${}_0T_9$	672	246	175	180	157–180
${}_0T_{10}$	619	238	167	173	188–250
${}_0T_{12}$	538	219	155	163	189–220
${}_0T_{14}$	477	200	145	155	200–270
${}_0T_{16}$	430	184	139	149	168–215
${}_0T_{20}$	360	160	129	142	175–249
${}_0T_{25}$	300	142	123	137	110–149
${}_0T_{30}$	258	136	119	134	111–142
${}_0T_{40}$	201	127	114	131	102–133
${}_0T_{50}$	164	119	112	131	108–130
${}_0T_{60}$	139	112	111	132	104–116
${}_0T_{70}$	121	105	111	· · ·	100
${}_0T_{80}$	107	98	111	· · ·	86–121
${}_0T_{85}$	101	95	111	· · ·	108
${}_0T_{110}$	79	90	111	· · ·	109

TABLE 9. Toroidal Overtone Q

Mode	Period, s	ABM	SL8	PREM	Data
${}_1T_7$	475	224	262	237	238*
${}_1T_{12}$	340	217	232	217	195*
${}_1T_{19}$	249	212	204	203	195*
${}_1T_{25}$	206	203	184	187	192*
${}_1T_{62}$	107	135	...	140	138*
${}_2T_{36}$	133	228	214	204	183*
${}_2T_{46}$	112	206	190	189	189
${}_2T_{49}$	107	198	181	183	207*
${}_2T_{54}$	100	186	172	173	144
${}_2T_{62}$	91	168	159	159	143
${}_3T_{26}$	147	243	241	220	264
${}_3T_{27}$	144	246	240	...	296
${}_3T_{30}$	134	251	239	219	215*
${}_3T_{53}$	91	215	214	...	236
${}_4T_{11}$	200	160	247	221	208
${}_4T_{47}$	170	146	254	...	204

*See text.

core would be a severe test of the suggested location of the Q_K band and Q_m for bulk dissipation.

RESULTS

Tables 5–10 and Figure 6 give the calculated Q for ABM and, for comparison, two frequency-independent Q models (SL8, *Anderson and Hart* [1978*b*]; PREM, *Dziewonski and Anderson* [1981]). The main differences of the absorption band model, compared with the constant Q models, are the higher theoretical values for ${}_0S_2$, ${}_0S_3$, and ${}_0S_4$ and the more rapid decrease of Q from ${}_0S_5$ to ${}_0S_{10}$. Unfortunately, there is considerable uncertainty in the Q values for the low-order spheroidal modes. The data are compiled from *Anderson and Hart* [1978*a*, *b*], *Chael and Anderson* [1982], *Nakanishi* [1979*a*], and *Dziewonski and Steim* [1982]. In general, the fit of ABM is as good as or better than the constant Q models.

The fundamental toroidal modes are given in Table 8. ABM has values appreciably higher than SL8 and PREM for modes ${}_0T_3$ to ${}_0T_{20}$. The toroidal overtones are given in Table 9.

The values for t_p* and t_s* (travel time over average Q) are given in Table 11 as a function of distance and period. At 100 s the Q_K contribution is small and $t_p^* \sim 1$ and $t_s^* \sim 4$-5, values which are commonly used in long-period waveform fitting. At high frequencies the predicted t^* values are much lower and are generally consistent with spectral studies [*Der and McElfresh*, 1980; *Clements*, 1982]. There are very few studies of t_s*. *Clements* [1982] gives values that mostly fall in the range of 0.8 to 1.6 s at periods near 1 s. ABM, Table 11, satisfies these observations. Note that $t_s^* < 4\ t_p^*$ at short periods because of the Q_K contribution. If there were no bulk absorption, t_p* (30°) at 1 s would be 0.32 s and the other t_p* values at short period would be correspondingly reduced. Such low values for t_p* have been reported for some regions, but average values seem to be somewhat higher. Note that t^* decreases gradually with frequency at the shorter distances. The study of t^* as a function of frequency and distance should allow better constraints to be placed on τ_1, for both Q_s and Q_K, as a function of depth.

The average Q values for the crust and upper mantle (<670 km), lower mantle (>670 km), and whole mantle are given in Table 3. Table 3 also gives the average Q of a ${}_0S_2$ type mode at tidal and Chandler periods, ignoring rigid body rotation and ocean effects.

Table 12 give a condensed summary of the fit of ABM to selected normal mode and surface wave Q data. Global

TABLE 10. High Q Modes

Mode	Period, s	ABM	SL8	PREM	Data
${}_1S_7$	604	315	473	372	484
${}_2S_4$	725	411	...	380	350
${}_3S_1$	1061	856	902	827	1020
${}_4S_3$	488	466	534	...	560
${}_4S_{23}$	170	241	287	...	312
${}_4S_{26}$	157	250	278	...	306
${}_5S_7$	304	480	589	493	496
${}_6S_1$	505	695	873	...	700
${}_0S_0$	1230	6107	4374	5328	5230
${}_1S_0$	614	1293	1180	1499	1970
${}_2S_0$	399	1243	1024	1241	1170
${}_3S_0$	306	873	851	1083	874
${}_4S_0$	244	862	945	969	989
${}_5S_0$	205	782	947	921	824
${}_6S_0$	174	689	1057	913	933

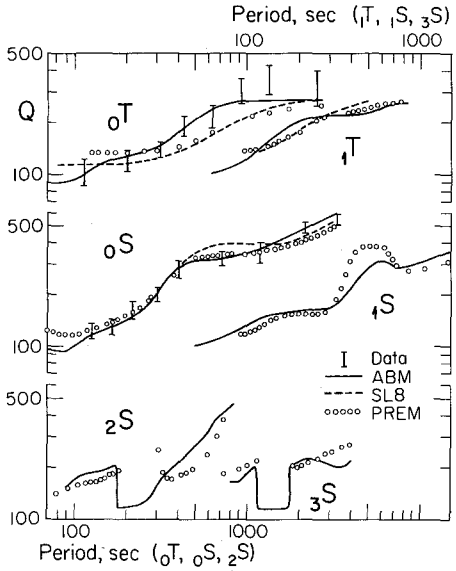

Fig. 6. Comparison of calculated Q values for ABM and two frequency-independent Q models, SL8 and PREM. The approximate range of the data for the fundamental modes is shown by vertical bars.

means for mantle Rayleigh waves are probably accurate to better than 5% [*Dziewonski and Steim*, 1982; *Chael and Anderson*, 1982]. Most of the other data has an estimated subjective uncertainty, in the context of global means, of about 20%. Since much of the published data have unknown uncertainties and are individual measurements rather than global means and since many measurements appear to be inconsistent [*Anderson and Hart*, 1978*a*], the choice of which data should be fit exactly and which should be fit approximately, or discarded, is somewhat arbitrary. At this stage in Q modeling, checking the consistency of the data against a theoretical model is as instructive as the more usual reverse procedure. A more complete comparison is given in Tables 5–11. A summary of body wave data is given in Table 13.

We conclude that ABM is an adequate fit to a variety of data over a broad frequency band. Our goal was to determine if a physically realistic model of the absorption band, with its attendant frequency dependence and large shifts with depth, could explain the surface wave and normal mode absorption spectrum. This goal was achieved. In addition, body wave data such as t_p*, t_s*, and $Q(ScS)$ are also satisfied by ABM, indicating that a very simple absorption band model can reconcile available data over a very broad frequency range.

Discussion

The absorption band for Q_s is centered at about 1-s period in the upper 400 km of the mantle with the maximum absorption at about 100 s. The band moves slightly to longer periods with increasing depth over this interval. This could be due to the effect of increasing pressure and decreasing tectonic stress. The band jumps to longer periods at about 400-km depth and gradually moves to longer periods with increasing depth. The location of the band in the lower mantle is determined from the long-period spheroidal modes. The very low-order spheroidal modes, $_0S_2$ to $_0S_5$, can only be satisfied, even with their large uncertainty, by moving the absorption band back to shorter periods at the base of the mantle. This gives a relatively low-Q zone at the base of the mantle for short-period body waves. This shift may be due to a high-temperature gradient or high stresses in D″, effects expected in a thermal and mechanical boundary layer at the base of a convecting lower mantle. Whole mantle convection is not implied by the presence of such a boundary layer.

There is much less control on Q_K. The assumption that bulk losses also satisfy the relaxation relations and that the Q_K absorption band is centered at short periods leads to the conclusion that the minimum Q_K is greater than the minimum Q_s. The outer core may have relatively high absorption for long-period body waves. With the placement of the Q_K band, $Q_p < Q_s$ at short periods at midmantle depths. This conclusion, however, rests on the assumption that $t_p^* > 0.6$ s at short periods. Low Q_p/Q_s ratios at short periods are predicted by the model and are consistent with available data. Unfortunately, global averages for t_p* and t_s* are not available.

Since most seismic data average over a large part of the mantle or core, the integrated effect leads to a mild frequency dependence over most of the seismic band. A stronger frequency dependence is predicted for the high-Q regions of

TABLE 11. t_p* and t_s* as Function of Distance and Period for Models ABM and the Frequency-Independent Q Model SL8

		Distance, deg						
	Wave	30	40	50	60	70	80	90
Period, s								
0.1	P	0.61	0.72	0.83	0.93	1.02	1.10	1.51
	S	0.99	0.97	0.93	0.89	0.87	0.85	1.97
1.0	P	0.65	0.67	0.66	0.65	0.66	0.67	1.14
	S	1.44	1.43	1.39	1.34	1.32	1.29	2.87
4.0	P	0.73	0.74	0.71	0.69	0.68	0.67	1.23
	S	1.93	1.97	1.96	1.95	1.93	1.91	3.81
10.0	P	0.68	0.71	0.72	0.71	0.72	0.72	1.32
	S	2.52	2.66	2.75	2.81	2.81	2.84	4.91
100.0	P	0.86	0.96	1.02	1.07	1.13	1.17	1.92
	S	3.82	4.22	4.55	4.84	5.10	5.35	8.00
Model SL8								
	P	0.91	1.02	1.04	1.04	1.06	1.06	1.12
	S	4.15	4.61	4.77	4.82	4.93	4.99	5.07

TABLE 12. Fit of Absorption Band Model to Selected Normal Data and Depth Range of Primary Sensitivity

Mode	Period, s	Q_{obs}	Percent ±	Q_{ABM}	Deviation, %	Region, km
			Shear Modes			
${}_0S_{70}$	134	120	5	121	−1	0–400
${}_0S_{30}$	262	179	5	177	1	200–700
${}_0S_{22}$	325	228	5	231	−1	300–800
${}_0S_{14}$	448	294	5	307	−4	600–1500
${}_0S_{10}$	580	320	5	319	0	800–2000
${}_0S_6$	964	343	20	350	−2	1500–2600
${}_0S_4$	1546	411	20	421	−2	1700–CMB
${}_0S_2$	3232	589	30	596	−1	2000–CMB
${}_0T_{85}$	101	108	20	95	12	0–100
${}_0T_{55}$	151	114	20	115	−1	0–200
${}_0T_{40}$	201	133	20	127	5	0–400
${}_0T_{32}$	244	133	20	134	−1	0–400
${}_1T_{62}$	107	138	20	135	2	0–700
${}_0T_{18}$	391	172	20	172	0	0–700
${}_2T_{49}$	107	207	20	198	4	0–1000
${}_1T_{25}$	206	192	20	203	−5	0–1000
${}_0T_{12}$	538	220	20	219	0	0–1000
${}_0T_8$	736	250	20	253	−1	0–1000
${}_0T_4$	1304	290	20	267	8	0–1700
${}_3T_{53}$	91	236	20	215	9	0–1700
${}_3T_{26}$	147	264	20	243	8	0–2400
${}_1T_7$	475	238	20	224	6	200–2400
${}_2S_{30}$	161	207	20	200	3	0–700
${}_2T_{57}$	98	170	20	174	−2	0–1000
${}_3T_{42}$	111	180	20	206	−14	0–1000
${}_3S_{20}$	217	222	20	229	−3	0–1000
${}_6S_{47}$	89	276	20	263	5	400–1700
${}_4S_{35}$	127	246	20	234	5	700–1500
${}_4S_{31}$	139	264	20	246	7	700–1500
${}_5S_{30}$	129	248	20	251	−1	600–1800
${}_5S_{25}$	143	231	20	227	1	600–1800
${}_4S_{21}$	181	231	20	275	−19	1000–2000
${}_4S_{19}$	192	291	20	218	25	1000–2000
${}_3S_{12}$	297	239	20	210	12	200-2400
			Compressional Modes			
${}_6S_{47}$	89	276	20	263	5	400–1700
${}_6S_{23}$	138	299	20	272	6	200–700
${}_2S_4$	726	350	5	411	−17	0–1000
${}_5S_7$	304	496	20	480	3	300–1500
${}_6S_0$	174	933	15	689	26	· · ·
${}_6S_1$	505	700	20	695	1	0–6371
${}_5S_0$	205	824	17	782	5	· · ·
${}_4S_0$	244	989	10	862	33	· · ·
${}_3S_0$	306	874	15	873	0	· · ·
${}_2S_0$	399	1170	15	1243	−6	· · ·
${}_1S_0$	614	1970	19	1293	34	1000–2500 4000–5500
${}_0S_0$	1230	5230	9	6107	−17	1000–5000

CMB is the core-mantle boundary region.

the earth. The deformational Q at tidal and Chandler periods is predicted to be somewhat less than for the mode ${}_0S_2$.

EPILOGUE

It should be obvious by now that the global Q problem is quite different from the travel time and eigenfrequency problem. The accuracy and quantity of the Q data are 1 to 2 orders of magnitude less than the data which are relevant to the determination of the elastic structure of the earth. The elastic problem is based on physics which has been developed for 300 years; the phenomenology of the process is not in doubt. In marked contrast the seismic data must be used not only to determine the anelastic structure of the earth but also to develop the phenomenology. For the absorption band modeling there is little previous experience to build on and no experimental guidelines on appropriate materials at relevant temperatures and frequencies. The next generation of Q models must take into account the frequency dependence of Q. These will represent a different class of models which cannot be viewed as small departures from previous frequency-independent Q models; they are not linearly close to models which have been developed from a different premise. The fundamental parameters are even different. In the frequency-independent Q models the question posed is: How does Q vary with depth? In the absorption band modeling there are a variety of approaches. We could assume, for example, that the shape of the absorption band is invariant with depth and ask: How does the mean relax-

TABLE 13. Fit of Absorption Band Model (ABM) to Selected Body Wave Data at Various Frequencies

Period, s	Data Range	ABM 30°	ABM 0°	Region
		t_p^*, s		
1	0.5–0.8	0.65		upper mantle
4	0.6–1.0	0.73		upper mantle
10	0.7–1.1	0.68		upper mantle
		t_s^*, s		
1	0.8–1.5	1.44		upper mantle
		Q, ScS		
1	300–750		477	whole mantle
4	220–400		360	whole mantle
10	180–300		280	whole mantle
100	140–200		176	whole mantle

ation time $\bar{\tau}$ vary with depth? Alternatively, we could assume a constant width for the absorption band and ask how does the modulus defect [*Minster and Anderson*, 1981] and Q_m, the minimum Q in the band, vary with depth? We have taken the first approach.

ABM is a relatively simple model. The mantle can be modeled by four or five layers of nearly constant properties (Figure 2). More complicated models, or models involving variable or multiple absorption bands, are not justified by the present data. However, different assumptions about the properties of the absorption bands will certainly lead to different-looking models.

APPENDIX: A DISCUSSION OF THE DATA

Even the best Q data probably have uncertainties of at least 5%. Most of the normal mode Q values are uncertain by 20–30%. Body wave Q and t^* data exhibit uncertainties and lateral variations of factors of 2 and 3. One could ask whether the present data make it possible to resolve anything. Shear attenuation varies over at least 3 orders of magnitude throughout the mantle and core and apparently can vary an order of magnitude from place to place and across the seismic band. In contrast, the seismic velocities vary by only a factor of 2 throughout the mantle and core, and lateral variations are of the order of 10% or less. Travel times and normal mode periods can be measured to better than 0.1%. It is meaningless to compare the absolute precicion of Q measurements to travel time or eigenfrequency precisions. The expected variation of the elastic properties and density are about 3 orders of magnitude less than the expected variation in Q, and therefore the precision of the data has to be correspondingly higher.

In global modeling one has to contend with a variety of data of variable accuracy and reliability. In addition, there is regional bias in body wave and surface wave studies. Thus it is difficult to compare body waves with free oscillations and to sort out frequency effects from radial and lateral variations.

There have been numerous studies of the attenuation of mantle Rayleigh waves over various great circle paths, and good global average values are now available for ${}_0S_9$ through ${}_0S_{76}$, which covers the period range from 634 to 125 s. The global means (Table 5) are probably good to better than 5% [*Dziewonski and Steim*, 1982; *Chael and Anderson*, 1982]. The absorption band model fits these data with an average error of 2.3%. The low-order modes, ${}_0S_2$ to ${}_0S_8$, periods greater than 700 s, are only excited by very large earthquakes, and there are consequently fewer studies of these modes and global coverage is poor. For these modes, a range of Q values is given in Table 5 which includes most of the observations. The range is of the order 20%.

For the spheroidal overtones (Tables 6 and 7) there are relatively few observations, and no global average can be constructed. When multiple observations, or observations of adjacent modes, are available, it appears that the uncertainties are of the order of 20 to 30%. There is also the possibility of mode misidentification [*Anderson and Hart*, 1978*a*].

Dziewonski and Anderson [1981] picked out what they felt where the most reliable overtone observations and assigned a subjective uncertainty, usually 20%. These modes are identified by asterisks in Tables 6 and 7. ABM fits these modes with an average error of 15%. When more than one observation of a mode is available, the range is tabulated.

The fundamental toroidal modes (Table 8) have been less studied than the spheroidal modes, and again, no global average or uncertainty can be estimated. Since averages are meaningless, we have tabulated the range in which most observations lie except for the cases where only a single observation is available. It is clear from Table 8 that more toroidal and Love wave Q data are desirable. The uncertainties in the fundamental toroidal mode Q appear to be of the order of 30%, and they appear to provide only a very weak constraint on mantle Q. They are not useless, however, since the models in Table 8 also vary by about 30% for periods between 360 and 1000 s. The frequency-independent Q models give values which generally lie outside the range of the data.

The toroidal overtones are given in Table 9. Again, the modes denoted by asterisks were used in the *Dziewonski and Anderson* [1981] inversion and have an assigned uncertainty of 20%. The model discussed in this paper fits these eight modes with an average error of 10%.

The high-Q modes are generally those modes which are most sensitive to Q_K and the core. These are tabulated in Table 10. These are usually based on a single observation, and no global average or uncertainty can be assigned. The main difference between the frequency-independent Q models (SL8 and PREM) and the absorption band model (ABM) is for the short-period radial modes, ${}_4S_0$, ${}_5S_0$, and ${}_6S_0$.

The normal modes alone do not yet provide a meaningful constraint on the frequency dependence of Q. The normal mode band is too narrow, the accuracy of the data is too low, and there is a trade-off between the depth dependence and the frequency dependence of Q. ScS data provide a useful constraint on Q_s for the whole mantle at various periods. Q_{ScS} increases from about 160 at 50 s to 210 at 10 s and 450 at 2 s [*Jordan and Sipkin*, 1977; *Sipkin and Jordan*, 1979; *Nakanishi*, 1979*b*; *Anderson and Hart*, 1978*a*]. The uncertainty in these values in the context of global means is about 30% if we consider the spread of available data.

The t_p^* at high frequency, 1–2 Hz, is typically 0.3 to 0.6 s [*Der and McElfresh*, 1980; *Clements*, 1982], much less than the values predicted from previous free oscillation constant Q models (Table 11). The t_s^* is about 0.6 to 1.2 in the same period range [*Clements*, 1982], again much lower than values predicted from free oscillation models. The ScS and t^* data suggest that Q increases rapidly with frequency at frequencies greater than 1 Hz.

Acknowledgments. We thank Robert Hart for use of a program and for help during the early stages of this project. Thorne Lay, Bernard Minster, Anton Hales, and Ichiro Nakanishi reviewed the manuscript and provided helpful comments. Research was supported by the Division of Earth Sciences, National Science Foundation grant EAR77-14675 and National Aeronautics and Space Administration grant NSG-7610, Contribution 3695, Division of Geological and Planetary Sciences, California Institute of Technology, Pasadena, California 91125.

REFERENCES

Anderson, D. L., Bulk attentuation in the Earth and viscosity of the core, *Nature, 285,* 204–207, 1980.

Anderson, D. L., and R. S. Hart, Attenuation models of the earth, *Phys. Earth Planet. Inter., 16,* 289–306, 1978*a*.

Anderson, D. L., and R. S. Hart, *Q* of the earth, *J. Geophys. Res., 83,* 5869–5882, 1978*b*.

Anderson, D. L., and J. B. Minster, The frequency dependence of *Q* in the earth and implications for mantle rheology and Chandler wobble, *Geophys. J. R. Astron. Soc., 58,* 431–440, 1979.

Anderson, D. L., and J. B. Minster, Seismic velocity, attenuation and rheology of the upper mantle, in *Source Mechanism and Earthquake Prediction,* edited by C. J. Allègre, pp. 13–22, Éditions du Centre National de la Recherche Scientifique, Paris, 1980.

Anderson, D. L., H. Kanamori, R. S. Hart, and H.-P. Liu, The earth as a seismic absorption band, *Science, 196,* 1104–1106, 1977.

Budiansky, B., and R. J. O'Connell, Bulk attenuation in heterogeneous media, in *Solid Earth Geophysics and Geotechnology,* edited by S. Nemat-Nasser, American Society of Mechanical Engineers, New York, 1980.

Chael, E., and D. L. Anderson, Global *Q* estimates from antipodal Rayleigh waves, *J Geophys. Res., 87,* 2840–2850, 1982.

Clements, J., Intrinsic *Q* and its frequency dependence, *Phys. Earth Planet. Inter., 27,* 286–299, 1982.

Choy, G., Theoretical seismograms of core phases calculated by frequency-dependent full wave theory, and their interpretation, *Geophys. J. R. Astron. Soc., 51,* 275–312, 1977.

Cormier, V., and P. Richards, Comments on 'The damping of core waves' *J. Geophys. Res., 81,* 3066–3068, 1976.

Der, Z., and T. W. McElfresh, Time domain methods, the values of t_p^* and t_s^* in the short-period band and regional variations of the same across the United States, *Bull. Seismol. Soc. Am., 70,* 921–924, 1980.

Doornbos, D. J., The anelasticity of the inner core, *Geophys. J. R. Astron. Soc., 38,* 397, 1974.

Dziewonski, A., and D. L. Anderson, Preliminary reference earth model, *Phys. Earth Planet. Inter., 25,* 297–356, 1981.

Dziewonski, A., and J. Steim, Dispersion and attenuation of mantle waves through wave-form inversion, *Geophys. J. R. Astron. Soc.,* in press, 1982.

Jordan, T., and S. Sipkin, Estimation of the attenuation operator for multiple *ScS* waves, *Geophys. Res. Lett., 4,* 167–170, 1977.

Kanamori, H., Spectrum of short-period phases in relation to attentuation in the mantle, *J. Geophys. Res., 72,* 2181–2186, 1967.

Kanamori, H., and D. L. Anderson, Importance of physical dispersion in surface-wave and free oscillation problems, Review, *Rev. Geophys. Space Phys., 15,* 105–112, 1977.

Kovach, R. L., and D. L. Anderson, Attenuation of shear waves in the upper and lower mantle, *Bull. Seismol. Soc. Am., 54,* 1855–1865, 1964.

Liu, H.-P., D. L. Anderson, and H. Kanamori, Velocity dispersion due to an elasticity: Implications for seismology and mantle composition, *Geophys. J. R. Astron. Soc., 47,* 41–58, 1976.

Lundquist, G. M., and V. C. Cormier, Constraints on the absorption band model of Q, *J. Geophys. Res., 85,* 5244–5256, 1980.

Minster, J. B., and D. L. Anderson, Dislocations and nonelastic processes in the mantle, *J. Geophys. Res., 85,* 6347–6352, 1980.

Minster, J. B., and D. L. Anderson, A model of dislocation-controlled rheology for the mantle, *Philos. Trans. R. Soc. London, 299,* 319–356, 1981.

Nakanishi, I., Phase velocity and *Q* of mantle Rayleigh waves, *Geophys. J. R. Astron. Soc., 58,* 35–59, 1979*a*.

Nakanishi, I., Attenuation of multiple *ScS* waves beneath the Japanese arc, *Phys. Earth Planet. Inter., 19,* 337–347, 1979*b*.

Qamar, A., and A. Eisenberg, The damping of core waves, *J. Geophys. Res., 79,* 758–765, 1974.

Sacks, I. S., *Q* structure of the inner and outer core (abstract), *Eos Trans. AGU, 53,* 601, 1972.

Sailor, R., and A. Dziewonski, Measurements and interpretation of normal mode attentuation, *Geophys. J. R. Astron Soc., 53,* 559–582, 1978.

Sipkin, S. A., and T. H. Jordan, Frequency dependence of Q_{ScS}, *Bull. Seismol. Soc. Am., 69,* 1055–1079, 1979.

Suzuki, Y., and R. Sato, Viscosity determination in the earth's outer core from *ScS* and *SKS* phases, *J. Phys. Earth, 18,* 15–170, 1970.

Zener, C., *Elasticity and Anelasticity of Metals,* Chicago Press, Chicago, Illinois, 1948.

(Received September 29, 1981;
revised February 10, 1982;
accepted February 26, 1982.)